DOI: 10.58895/ksp/1000044906-2 erschienen in:

OCM 2015 - 2nd International Conference on Optical Characterization of Materials, March 18th – 19th, 2015, Karlsruhe, Germany : Conference Proceedings

DOI: 10.58895/ksp/1000044906 | https://www.ksp.kit.edu/site/books/m/10.58895/ksp/1000044906/

Prediction of lamb eating quality using hyperspectral imaging

Tong Qiao, Jinchang Ren, Jaime Zabalza and Stephen Marshall

Centre for excellence in Signal and Image Processing (CeSIP),
Department of Electronic and Electrical Engineering,
University of Strathclyde, Glasgow, UK.
(Corresponding author: jinchang.ren@strath.ac.uk)

Abstract Lamb eating quality is related to 3 factors, which are tenderness, juiciness and flavour. In addition to these factors, the surface colour of lamb could influence the purchase decision of consumers. Objective quality evaluation approaches, like near-infrared spectroscopy (NIRS) and hyperspectral imaging (HSI), have been proved fast and non-destructive in assessing beef quality, compared with conventional methods. However, rare research has been done for lamb samples. Therefore, in this paper the feasibility of HSI for evaluating lamb quality is tested. A total of 80 lamb samples were imaged using a visible range HSI system and the spectral profiles were used for predicting lamb quality related traits. For some traits, noises were removed from HSI spectra by singular spectrum analysis (SSA) for better performance. Support vector machine (SVM) was employed to construct prediction equations. Considering SVM is sensitive to high dimensional data, principal component analysis (PCA) was applied to reduce the dimensionality first. The prediction results suggest that HSI is promising in predicting lamb eating quality.

1 Introduction

Similar to beef production, lamb also plays an important role in UK agriculture, contributing over 10% of total live stock output [1]. Eating quality of lamb is related to many chemical and physical properties. It was found that 3 key factors, which are tenderness, juiciness and flavour, have an influence on the repurchase behaviour of consumers [2]. In addition to those factors, meat surface colour is considered as the most

significant factor determining retail selection of consumers [3]. Usually, evaluation of the above mentioned traits is achieved by measuring some mechanical properties of the meat sample, which can be costly, destructive and time-consuming.

Over the past a few decades, some objective approaches for predicting meat quality traits have been developed. Some examples include ultrasound, near infrared spectroscopy (NIRS), multispectral imaging, hyperspectral imaging (HSI) and various computer vision techniques. Among these approaches, NIRS is the most widely used technique for meat quality evaluation due to its simplicity, rapidity and effectiveness, but one major drawback of this technique is its low spatial resolution for analysing non-homogeneous composition of meat samples [4]. To this end, HSI integrating both spatial and spectral information has emerged, which shows great potential in remote sensing applications [5, 6]. In recent years, some researchers have demonstrated that HSI has some promise for predicting beef quality traits [7]. But to our knowledge, limited research has been conducted using HSI to predict quality traits of lamb samples.

The objective of the paper is to investigate the feasibility of HSI in predicting lamb quality related traits. In this study, ultimate pH was measured as the flavour reference and MIRINZ shear force (SF) was measured as the tenderness reference. Surface colour was measured in CIE (Commision Internationale de l'Eclairage) colour space as L*, a* and b*, where L* is the lightness, a* is redness and b* is yellowness. The prediction equation was constructed by the support vector machine (SVM) on a calibration set and the performance was assessed on the additional validation set. Details will be explained in following sections.

2 Materials and methods

2.1 Lamb sample preparation and image collection

A total of 80 lamb samples were purchased from a commercial abattoir in Scotland. Storing at $3 \pm 2\,^{\circ}\mathrm{C}$ for 7 days after being slaughtered, left lamb loins were removed from packaging. After blooming for 2 minutes [8], HSI samples were collected using a push-broom HSI system (Gilden photonics) with wavelength ranging from 400 to 862.90 nm at a spectral

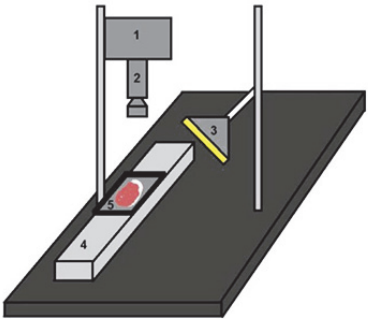

Figure 2.1: Schematic diagram of the HSI system: components 1-5 refer to the CCD camera, spectrograph and lens, halogen lamp, sliding track and scanning tray, respectively.

resolution of about 2.5 nm. Figure 2.1 shows a schematic diagram of the imaging system.

2.2 Measurements of quality related traits

Right after imaging, ultimate pH was determined by probing into the lamb sample derectly using a calibrated Hanna pH meter with a glass electrode (HI 99613). The surface colour was measured in the L*a*b* scale with a Minolta CR-410 colourimeter, where the machine is set to take 3 scans and then average them. Then, each lamb sample was labelled, vacuum packaged and frozen at $-30\,^{\circ}$C to prevent from further ageing. On the night before tenderness measurement, samples were placed in plastic bags and sub-merged in a water bath until reaching an internal temperature of $70\,^{\circ}$C and then chilled in the fridge. On the following day, 10 sub-samples with a 10 mm $\times$ 10 mm cross section were prepared parallel with the muscle fibre axis. All sub-samples were then sheared orthogonal to the fibre axis with a Tenderscot tenderometer (Pentland Precision Engineering Ltd) with a wedge shaped tooth according to the MIRINZ protocol [9]. The peak force was extracted during each shear process and the average value of 10 measurements is considered as the MIRINZ SF. Therefore, there are 5 lamb quality related traits in total for each sample, which are pH, L*, a*, b* and MIRINZ SF.

2.3 HSI data pre-processing

During the imaging process, reflectance of the sample was acquired by the HSI system. But before that, the HSI system has to be calibrated using a white reference image (nearly 100% reflectance) and a dark reference image (0% reflectance), which are 2 extreme illumination conditions. The reason is that the 'dark current' generated from thermal effects of the detectors should be deducted from the produced signal. Thus, the calibration procedures make sure that the sample reflectance is separated from system responses [7]. The following equation shows how the calibrated reflectance is achieved,

$$R = \frac{I-B}{I_0-B}, \tag{2.1}$$

where R is the calibrated reflectance image at one spectral band, I is the raw image at that band, B is the dark reference image and I_0 is the white reference image.

For each hypercube, there are 250 spectral bands acquired, while not all of these bands contain useful information. By removing needless spectral bands, the working wavelength for HSI spectra is 469.47 nm - 862.90 nm.

In order to save computing time, for each lamb sample, a region of interest (ROI) with size of 200 $\times$ 100 pixels was mainly selected from the lean part and then the median reflectance value at each spectral band was calculated to achieve the median reflectance spectrum. This process is illustrated in Figure 2.2. As suggested by other researchers, reflectance spectra (R) should be converted to absorbance (A) by logarithm transformation to linearise the relationship between the concentration of an absorbing compound and the absorption spectrum [10], where the equation is shown below,

$$A = \log_{10}\left(\frac{1}{R}\right) \tag{2.2}$$

As a relatively new technique, singular spectrum analysis (SSA), which is commonly used for time series analysis and forecasting, was applied to HSI absorbance spectra for de-noising. Based on the singular value decomposition, it is able to decompose the original spectrum into a few components, including the 'clean' spectrum, a few oscillations and

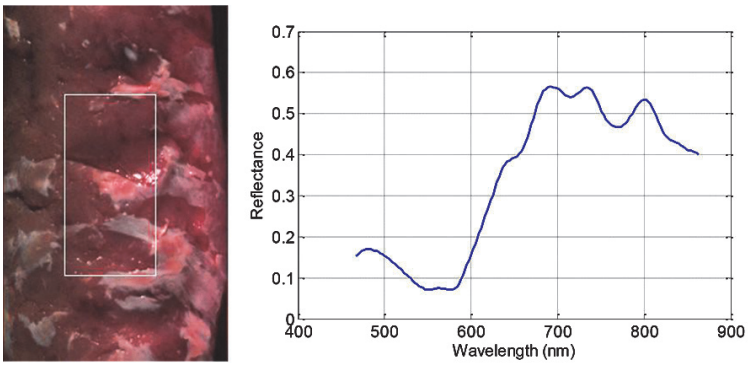

Figure 2.2: HSI median reflectance spectrum extraction. (a) Pseudo colour image of one lamb sample, with ROI marked by the white frame. (b) The median reflectance spectrum of the same sample.

noises. Details of the algorithm can be found in [11]. By reconstructing the spectrum with the first component, subtle noises can be discarded. For the same sample shown in Figure 2.2, the absorbance spectra without SSA and with SSA applied are plotted in Figure 2.3.

2.4 Regression analysis

A variety of statistical regression methods could be applied to construct prediction equations, including multiple linear regression, partial least squares regression (PLSR), principal components regression (PCR) and neural networks [4]. For predicting meat related traits, PLSR is the most common regression approach that researchers choose to build prediction models with NIRS [12–16]. However, PLSR is designed based on the linear algorithm so that the best performance might only be achieved when there is a linear relationship between spectra and quality traits [17], which is not applicable in our study. Therefore, instead of using PLSR, SVM was employed to build regression models. Results in [18] proved that SVM outperforms PLSR for beef quality evaluation using NIRS.

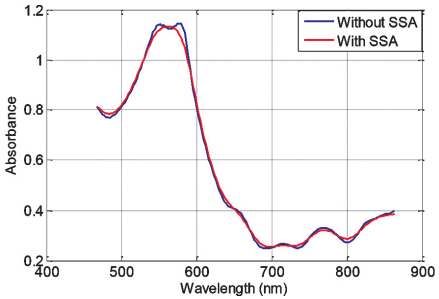

Figure 2.3: HSI absorbance spectrum without SSA applied (blue line) and HSI absorbance spectrum with SSA applied (red line).

The outstanding performance of SVM has been verified in many applications associated with HSI. However, a problem of SVM is that it is sensitive to the curse of dimensionality [19]. As a result, a commonly adopted feature extraction technique, principal component analysis (PCA) [20, 21], is used to reduce the dimensionality of HSI cubes. In this way, only a small amount of features could explain the whole dataset and the rest can be discarded.

With lower dimensional data, SVM could be applied to construct prediction models. For both classification and regression problems, SVM maps the data to a high dimensional feature space using kernel function. Then it is easy to separate the data by a maximal margin hyperplane. As a popular kernel function, the radial basis function (RBF) kernel was chosen. Optimal parameters were tuned using the grid search with 4-fold cross-validation to avoid model over-fitting.

3 Results and conclusion

80 lamb samples were split into the calibration set and the validation set, where prediction models were learnt from the calibration set and verified on the validation set. In this way, the ability of HSI for predicting quality of unknown lamb samples could be tested. In order to split the dataset, each quality trait was sorted in the ascending order. By selecting every 4th sample into the validation set, the rest of data which contain the interleaving 3 samples were allocated to the calibra-

Table 2.1: Summary statistics of all quality traits, including mean, standard deviation (SD) and range, where subscripts cal and val represent the calibration set and the validation set respectively.

Trait	n_{cal}	$Mean_{cal}$	SD_{cal}	$Range_{cal}$	n_{val}	$Mean_{val}$	SD_{val}	$Range_{val}$
pH	60	5.59	0.07	5.46 - 5.90	20	5.61	0.12	5.48 - 6.08
L*	60	41.47	1.83	36.69 - 46.64	20	41.83	2.31	38.74 - 49.63
a*	60	23.28	0.91	20.44 - 25.37	20	23.77	0.83	22.28 - 25.71
b*	60	7.77	0.58	5.89 - 9.15	20	7.85	0.57	7.02 - 9.17
SF	60	5.20	1.36	2.87 - 9.38	20	5.49	1.92	3.43 - 11.99

tion set [22]. This process makes sure that the validation set is a representative of the calibration set, with similar mean, standard deviation (SD) and range. Statistics of each quality trait are shown in Table 12.1. The unit for MIRINZ SF is kilogram force (kgF). The HSI performance for predicting lamb quality is evaluated quantitatively by the coefficient of determination (R^2) and the ratio of performance deviation (RPD). Equations for these metrics are given below:

$$R^2 = 1 - \frac{\sum_{i=1}^{n} (y_i - f_i)^2}{\sum_{i=1}^{n} (y_i - \bar{y})^2}, \tag{2.3}$$

$$RPD = \frac{SD}{RMSE} = \frac{SD}{\sqrt{\frac{\sum_{i=1}^{n} (y_i - f_i)^2}{n}}}, \tag{2.4}$$

where y_i is the original quality trait value, f_i is the predicted value, $\bar{y}$ is the mean of all original trait values, n is the sample number and $RMSE$ is the root-mean-square error in the investigated set. The coefficient of determination ranges from 0 to 1, where 0 represents a poor correlation between the predicted trait values and the reference trait values and 1 standards for a high degree of correlation. The number of principal components was tried from 5 to 50 in a step of 5, and both raw HSI absorbance spectra and SSA-treated absorbance spectra were tested. Combinations of best prediction results are shown in Table 12.2, where A stands for raw absorbance spectra and A + SSA means SSA-treated absorbance spectra.

Table 2.2: Performance for predicting quality traits in lamb using the visible range HSI system.

Trait	Pre-treatment	No. of principal components	R^2_{cal}	$RMSE_{cal}$	R^2_{val}	$RMSE_{val}$	RPD_{val}
pH	A	45	0.54	0.06	0.38	0.11	1.07
L*	A	15	0.83	0.67	0.77	1.34	1.72
a*	A + SSA	40	0.95	0.22	0.48	0.76	1.09
b*	A + SSA	15	0.83	0.34	0.26	0.50	1.13
SF	A + SSA	40	0.82	0.69	0.41	1.52	1.26

As the study is to test the ability of HSI in predicting unknown lamb quality for on-line use, the results of the extra validation set are particularly important. For the prediction of ultimate pH, R^2_{val} is higher than those reported in [1] ($R^2_{cv} = 0.03 - 0.19$). For colour parameters and MIRINZ SF prediction, limited research has been found on lamb. Nevertheless, our results agree with those predicted with beef sample using NIRS [12–16], whose average R^2 values are 0.76 and 0.44 for L* and a*. However, our result of b* is poorer than that of others ($R^2 = 0.57$), which may be due to variation between different samples. Similarly, we compare the MIRINZ SF with Warner-Bratzler SF predicted by others on beef sample. It is found that the average R^2 of their research is 0.30, which is lower than ours ($R^2_{val} = 0.41$).

In conclusion, this paper has demonstrated that HSI could be promising in offering additional information for predicting lamb quality, which might bring beneficial to lamb industries in the future.

4 Acknowledgement

This project is funded by Quality Meat Scotland (QMS) and University of Strathclyde. Authors would like to thank Dr. Cameron Craigie and Scotland's Rural College (SRUC) for helping preparing the data.

References

1. S. Andrés, I. Murray, E. Navajas, A. Fisher, N. Lambe, and L. Bünger, "Prediction of sensory characteristics of lamb meat samples by near infrared reflectance spectroscopy," *Meat Science*, vol. 76, no. 3, pp. 509–516, 2007.
2. L. Jeremiah and D. Phillips, "Evaluation of a probe for predicting beef tenderness," *Meat Science*, vol. 55, no. 4, pp. 493–502, 2000.
3. L. Jeremiah, Z. Carpenter, and G. Smith, "Beef color as related to consumer acceptance and palatability," *Journal of Food Science*, vol. 37, no. 3, pp. 476–479, 1972.
4. M. Prevolnik, M. Candek-Potokar, and D. Skorjanc, "Ability of nir spectroscopy to predict meat chemical composition and quality: a review," *Czech Journal of Animal Science-UZPI (Czech Republic)*, 2004.
5. J. Ren, J. Zabalza, S. Marshall, and J. Zheng, "Effective feature extraction and data reduction in remote sensing using hyperspectral imaging," *Signal Processing Magazine, IEEE*, vol. 31, no. 4, pp. 149–154, July 2014.
6. T. Qiao, J. Ren, M. Sun, J. Zheng, and S. Marshall, "Effective compression of hyperspectral imagery using an improved 3d dct approach for land-cover analysis in remote-sensing applications," *International Journal of Remote Sensing*, vol. 35, no. 20, pp. 7316–7337, 2014.
7. G. K. Naganathan, L. M. Grimes, J. Subbiah, C. R. Calkins, A. Samal, and G. E. Meyer, "Visible/near-infrared hyperspectral imaging for beef tenderness prediction," *Computers and Electronics in Agriculture*, vol. 64, no. 2, pp. 225–233, 2008.
8. S. Shackelford, T. Wheeler, and M. Koohmaraie, "On-line classification of us select beef carcasses for longissimus tenderness using visible and near-infrared reflectance spectroscopy," *Meat Science*, vol. 69, no. 3, pp. 409–415, 2005.
9. A. Frazer, "New zealand tenderness and local meat quality mark programmes," in *Proceedings of the meat quality and technology transfer workshop, 43 rd International congress of meat science and technology, July–August, Auckland, New Zealand*, 1997, pp. 37–51.
10. S. Rust, D. Price, J. Subbiah, G. Kranzler, G. Hilton, D. Vanoverbeke, and J. Morgan, "Predicting beef tenderness using near-infrared spectroscopy," *Journal of Animal Science*, vol. 86, no. 1, pp. 211–219, 2008.
11. J. Zabalza, J. Ren, Z. Wang, S. Marshall, and J. Wang, "Singular spectrum analysis for effective feature extraction in hyperspectral imaging," *Geoscience and Remote Sensing Letters, IEEE*, vol. 11, no. 11, pp. 1886–1890, Nov 2014.

12. S. Andrés, A. Silva, A. L. Soares-Pereira, C. Martins, A. Bruno-Soares, and I. Murray, "The use of visible and near infrared reflectance spectroscopy to predict beef m. longissimus thoracis et lumborum quality attributes," *Meat Science*, vol. 78, no. 3, pp. 217–224, 2008.

13. A. Cecchinato, M. De Marchi, M. Penasa, A. Albera, and G. Bittante, "Near-infrared reflectance spectroscopy predictions as indicator traits in breeding programs for enhanced beef quality," *Journal of Animal Science*, vol. 89, no. 9, pp. 2687–2695, 2011.

14. B. Leroy, S. Lambotte, O. Dotreppe, H. Lecocq, L. Istasse, and A. Clinquart, "Prediction of technological and organoleptic properties of beef longissimus thoracis from near-infrared reflectance and transmission spectra," *Meat Science*, vol. 66, no. 1, pp. 45–54, 2004.

15. N. Prieto, S. Andrés, F. J. Giráldez, A. Mantecón, and P. Lavín, "Ability of near infrared reflectance spectroscopy (nirs) to estimate physical parameters of adult steers (oxen) and young cattle meat samples," *Meat Science*, vol. 79, no. 4, pp. 692–699, 2008.

16. N. Prieto, D. Ross, E. Navajas, G. Nute, R. Richardson, J. Hyslop, G. Simm, and R. Roehe, "On-line application of visible and near infrared reflectance spectroscopy to predict chemical-physical and sensory characteristics of beef quality," *Meat Science*, vol. 83, no. 1, pp. 96–103, 2009.

17. M. Kamruzzaman, G. ElMasry, D. W. Sun, and P. Allen, "Prediction of some quality attributes of lamb meat using near-infrared hyperspectral imaging and multivariate analysis," *Analytica Chimica Acta*, vol. 714, pp. 57–67, 2012.

18. T. Qiao, J. Ren, C. Craigie, J. Zabalza, C. Maltin, and S. Marshall, "Quantitative prediction of beef quality using visnir spectroscopy with large data samples under industry condictions," *Journal of Applied Spectroscopy*, vol. 82, no. 1, January 2015.

19. F. Melgani and L. Bruzzone, "Classification of hyperspectral remote sensing images with support vector machines," *Geoscience and Remote Sensing, IEEE Transactions on*, vol. 42, no. 8, pp. 1778–1790, 2004.

20. J. Zabalza, J. Ren, J. Ren, Z. Liu, and S. Marshall, "Structured covariance principal component analysis for real-time onsite feature extraction and dimensionality reduction in hyperspectral imaging," *Applied Optics*, vol. 53, no. 20, pp. 4440–4449, 2014.

21. J. Zabalza, J. Ren, M. Yang, Y. Zhang, J. Wang, S. Marshall, and J. Han, "Novel folded-pca for improved feature extraction and data reduction with hyperspectral imaging and sar in remote sensing," *ISPRS Journal of Photogrammetry and Remote Sensing*, vol. 93, pp. 112–122, 2014.

22. P. Williams and K. Norris, *Near-infrared technology in the agricultural and food industries*. American Association of Cereal Chemists, Inc., 1987.